



Sharif University of Technology

Scientia Iranica

Transaction F: Nanotechnology

www.scientiairanica.com



Effects of bioglass nanoparticles on bioactivity and mechanical property of poly(3-hydroxybutirate) scaffolds

H. Hajiali^{a,b}, S. Karbasi^{b,*}, M. Hosseinalipour^a and H.R. Rezaie^a

a. Biomaterial Group, School of Metallurgy and Materials Engineering, Iran University of Science and Technology (IUST), Tehran, Iran.

b. Medical Physics and Biomedical Engineering Group, School of Medicine, Isfahan University of Medical Sciences, Isfahan, Iran.

Received 11 August 2012; received in revised form 12 November 2012; accepted 25 May 2013

KEYWORDS

Bone tissue engineering;
PHB;
Nanocomposite;
Mechanical properties;
Bioactivity.

Abstract. The development of composite scaffold materials in bone tissue engineering is gaining appeal, as the beneficial properties of two or more types of material can be compounded together to better respond to the mechanical and physiological demands of the host tissue. In this study, poly (3-hydroxybutyrate) was reinforced with a different weight ratio of nanobioglass (0, 2.5, 5, 7.5 and 10 wt%). The nanocomposite scaffolds were successfully prepared by the salt leaching process with various volume fractions of porosities (70, 80 and 90 wt% of NaCl). The results of our studies showed a favorable interaction between polymer and bioglass nanoparticles, which improved interfaces and mechanical properties, especially in samples which were prepared with 70 wt% NaCl. The Young's modulus of samples ranged from 7.23 MPa to 48.27 MPa, which were in the range of the Young's modulus of cancellous bone. The analysis results of samples which were immersed in SBF showed that hydroxyapatite formed on the nanocomposite scaffold surfaces, and they exhibited high bioactivity compared to the pure PHB scaffolds. In this study, nanobioglass, as a reinforcement phase with low mass fraction, is shown to be more effective than micro-materials with high mass fraction.

© 2013 Sharif University of Technology. All rights reserved.

1. Introduction

Recently, tissue engineering has been widely probed as a promising method towards the regeneration of tissue. Bone tissue engineering has developed biodegradable scaffolds as bone graft substitutes for healing large bone defects [1]. Poly (3-hydroxybutyrate) (PHB) exhibits an excellent biocompatibility with various cell lines and, therefore, it can be applied to a variety of medical applications [2].

PHB and bioactive inorganic phases (e.g. hydroxyapatite, wollastonite and bioglass) have been

combined to produce composite scaffolds which have better strength and bioactivity [3,4]. The greater specific surface area of the nanoparticles should lead to higher interface effects and also cause improved bioactivity and mechanical properties when compared to micro size particles [5-8].

Nejati et al. showed that nano-hydroxyapatite in Poly (L-Lactide Acid) (PLLA) composite has higher compressive strength and modulus than microcomposite [9]. Addition of hydroxyapatite nanoparticles to PLLA scaffolds has also been reported to assist the scaffolds in maintaining anisotropic and regular pore structure, compared to irregular pore structure, due to the addition of μm -sized hydroxyapatite [6]. Boccacini et al. showed that bioglass exhibited several advantages (excellent osteoconductivity and high bioactivity) in

*. Corresponding author. Tel.: +98 311 7922459;
Fax: +98 311 6688597
E-mail address: karbasi@med.mui.ac.ir (S. Karbasi)

comparison to other bioactive ceramics, e.g. sintered hydroxyapatite [10]. Misra and co-workers showed that nano-bioactive glass in PHB composite films resulted in a significant increase in Young's modulus and bioactivity compared to the value of the microcomposite film [5]. In addition, use of nanoparticles in a polymeric matrix closely mimics the structure of natural bone [11].

Most work on this class of composites has been carried out using commercial bioactive glass microparticles (45S5) as fillers in composite film structures. Thus, the objective of this study is to fabricate nanocomposite scaffolds with improved mechanical properties and interconnected porous structures for bone tissue engineering applications, using the other class of bioactive glass nanoparticles.

2. Materials and methods

2.1. Materials

Poly (3-hydroxybutyrate) was purchased from Sigma-Aldrich (USA, CAS NUMBER: 26063-00-3, LOT NUMBER: S68924-099), and NaCl and chloroform from Merck (Germany). Also, Tetraethylorthosilicate (TEOS, Merck) as the silica precursor, Hydrogen ammonium phosphate (Merck) as the phosphorus precursor, and Calcium nitrate (Merck) as the calcium precursor were prepared.

2.2. Preparation of nanobioglass

Nanobioglass was produced as described by Fathi and Doostmohammadi [12]. The size of bioactive glass powder was less than 100 nm. The TEOS and ethanol were mixed and then distilled water was added to the solution using a magnet stirrer and allowed to combine until the solution became clear. The H₂O to TEOS molar ratio was 12:1. After 30 minutes, hydrogen ammonium phosphate was added to the stirred solution and, after another 20 minutes, calcium nitrate was added and the solution was stirred for an additional hour. On completion of the hydrolysis procedure, the sols were aged in a drying oven at 50°C to reach a high viscosity near the gelling point. The composition of the prepared bioactive glass is shown in Table 1.

2.3. Preparation of scaffolds

PHB/bioglass nanocomposite scaffolds were prepared using salt-leaching techniques. Briefly, 2 g PHB and 0, 0.05, 0.1, 0.15 and 0.2 g nanobioglass were dissolved in chloroform with 6% w/v and refluxed at 60°C for 6 hours. Then, they were sonicated for 30 min using a sonicating probe. Subsequently, the solution was

Table 1. Composition of nanobioglass.

	CaO	SiO ₂	P ₂ O ₅
Composition of nanobioglass	57.44%	35.42%	7.15%

Table 2. Composition of prepared scaffolds.

Samples composition						
		Wt% of nanobioglass				
		0%	2.5%	5%	7.5%	10%
Wt% of NaCl	90%	S1	S2	S3	S4	S5
	80%	S6	S7	S8	S9	S10
	70%	S11	S12	S13	S14	S15

poured onto a bed of sieved sodium chloride particles, 250 to 300 μm, and the sodium chloride: polymer weight ratios were 90/10, 80/20 and 70/30. The scaffolds were placed under vacuum in a desiccator for 24 hrs for the solvent to evaporate completely. Then, it was rinsed with large amounts of distilled water for leaching the salt. After the salt-leaching process was completed, the micro-porous polymer scaffolds were obtained and vacuum dried (Table 2).

2.4. Scanning Electron Microscopy (SEM)

Some scaffolds were broken in liquid nitrogen to probe the cross section area. Then, the samples were mounted on aluminum stumps, coated with gold in a sputtering device, and then examined using a scanning electron microscope for pore structure study. SEM images were taken at various magnifications and acceleration voltages (max. of 15 kV) to avoid beam damage to the polymer.

2.5. ATR-FTIR analysis

To characterize the surface of the modified samples, attenuated total reflectance Fourier transform infrared (ATR-FTIR) analysis was performed using a FT-IR instrument (BRUKER) with a ZnSe prism.

2.6. Determination of porosity

The weight (Wd) and volume (V) of the dried scaffolds were measured and then the scaffolds were immersed in de-ionized water overnight. Afterwards, the weight of wet scaffolds (Ww) was measured. The weight of water absorption in the pores of the scaffolds was determined by subtracting the scaffolds' dry weight (Wd) from Ww . The voids of the porous scaffolds can be equivalent to the volume of water absorption, and the amount of porosity was calculated as follows [13]:

$$P\% = \left(\frac{Ww - Wd}{V} \right) 100. \quad (1)$$

2.7. Mechanical test

Sheet-like rectangular scaffolds at compositions listed in Table 1 were used as samples for the tensile test. The tensile test, using a universal testing machine, was performed on a 10 × 50 mm rectangular specimen (gauge length = 30 mm) with a 10 N load-cell. The crosshead speed used for all specimens was 1 mm/min. After measuring the stresses and strains of 15 scaffolds,

the Young's modulus of each scaffold was calculated using:

$$E = \frac{Pl}{\delta l t d}, \quad (2)$$

where E , P , l , δl , t and d represent Young's modulus, stress, length, variation of length, thickness and width of the sheet, respectively.

2.8. *In vitro* bioactivity test

In vitro bioactivity, studies were carried out using standard Simulated Body Fluid (SBF) based on the formulation and method developed by Kokubo and Takadama [14], which contains inorganic ion concentrations similar to those of human blood plasma. The SBF was adjusted to physiological pH (pH 7.4) by HCl at 37°C and buffered by tris (hydroxyl-methyl) amino-methane.

The scaffolds were immersed in SBF for up to 4 weeks. The SBF solution was stirred and refreshed every two days in the first week and then weekly for the remaining time. During the immersion period, the scaffolds were kept at 37°C in a humidified incubator, and the pH of SBF was controlled everyday to maintain it at a constant range (pH 7.3–7.4) by HCl and Tris. After 4 weeks, the scaffolds were taken out from the SBF and gently rinsed with de-ionized water. They were dried at room temperature and, then, analyzed by scanning electron microscopy coupled with energy dispersive spectroscopy (SEM/EDS, Leica Cambridge S360).

3. Results and discussion

3.1. Scaffolds characterization

In our previous study, nanocomposite scaffolds were investigated by high magnification SEM, FTIR and DTA [13]. The microstructure of scaffolds that were prepared by various weight ratios of NaCl is shown in Figure 1(a)–(f). The SEM images demonstrated uniform porosities of 250–300 μm pore size, which is suitable for osteoblast migration [15,16]. Figure 1(a) and (b) shows the scaffold prepared by 90 wt% NaCl, and the high pore interconnectivity essential for cell migration, waste removal and nutrient supply to the scaffold in bone tissue engineering [17] can be seen. The scaffolds which were prepared by 80 and 70 wt% NaCl are shown in Figure 1(c), (d), (e) and (f), respectively. The images show that the pore walls were thicker, and the interconnectivity and porosity was reduced by decreasing the NaCl amount in the scaffold preparation.

The samples with bioglass nanoparticles were investigated using SEM under higher magnification in order to observe their structure in more detail. The results have been shown in Figure 1(g). As can be seen,

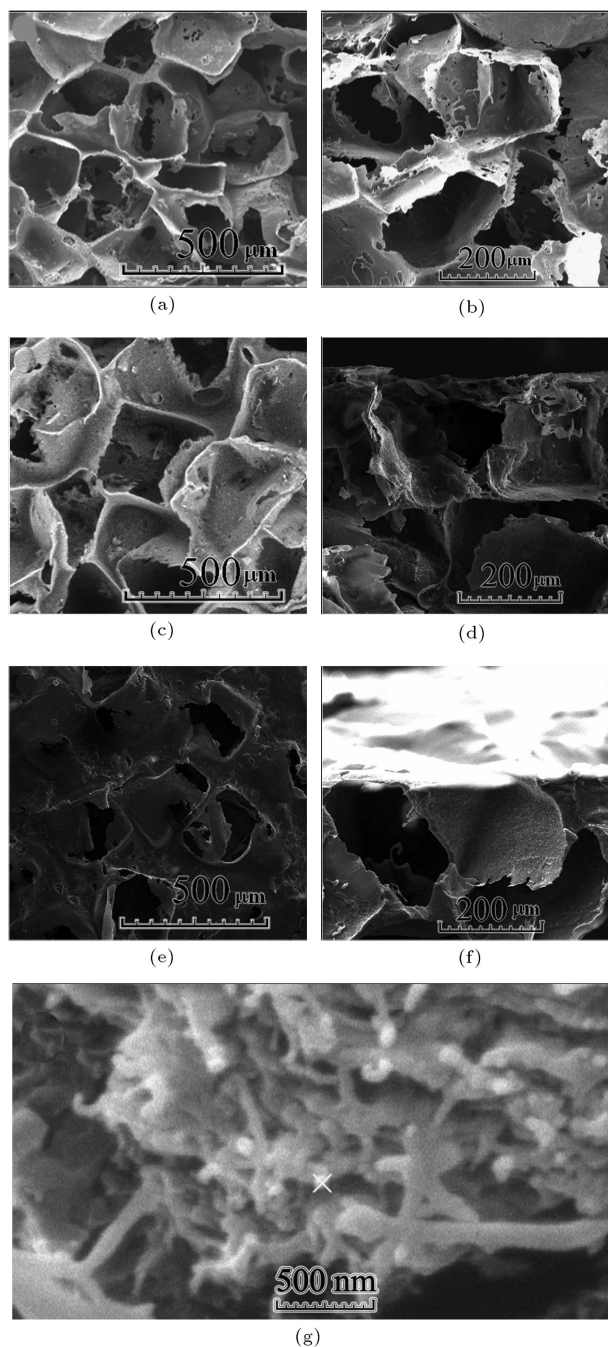


Figure 1. SEM of nanocomposite scaffolds which were prepared with various porosity: (a) The surface and (b) cross section of scaffold which was prepared by 90 wt% NaCl; (c) the surface and (d) cross section of scaffold which was prepared by 80 wt% NaCl; (e) the surface and (f) cross section of scaffold which was prepared by 70 wt% NaCl; and (g) the SEM of nanocomposite 30000 \times magnification. The size of marked nanobioglass is 53 nm.

the particles are constructed by a relatively ordered array of nanoparticles in the polymer solution and the prepared nano composites exhibit a rough surface that may improve cell attachment. The size of nanoparticles marked in Figure 1(g) is about 53 nm, regarding

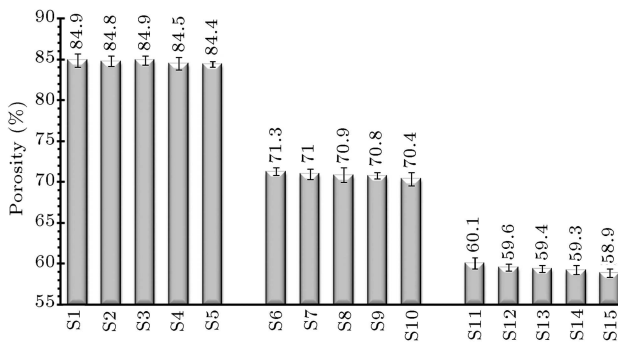


Figure 2. Porosity of scaffolds. The data: $n = 3$, error bars = \pm SD.

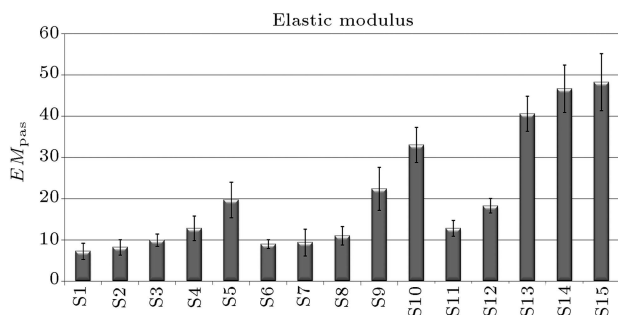


Figure 3. Young's modulus of scaffolds. The data: $n = 3$, error bars = \pm SD).

the primary particle size of nanobioglass [12], which exhibits the lack of agglomeration.

The porosity of the scaffolds was assessed and the results are shown in Figure 2. The porosities and pore sizes of the scaffolds can easily be controlled by variations in salt concentration and the salt particle size range. The salt weight percentage (relative to the polymer) varies between 70, 80 and 90 wt%. Depending on NaCl density, the resulting porosities of the porous structures were between 58.9 and 84.9%. The figure shows that it is possible to prepare porous scaffolds with a range of porosities up to 80% or more. At higher concentrations, however, the salt particles could readily be extracted. This implies that at higher salt concentrations (and higher porosities), an interconnected pore network was obtained.

3.2. Mechanical properties of scaffolds

Young's modulus was calculated for each scaffold and the results are shown in Figure 3. The Young's modulus of the scaffolds decreased with increasing porosity. It is an acceptable phenomenon based on the theory [18]. The Young's modulus of the scaffolds containing nanobioglass is higher than the modulus of neat PHB scaffolds, and increases with increasing nanobioglass mass fraction. As shown in Figure 3, the Young's modulus of S15 (a composition of PHB and 10 wt% nanobioglass with 58.9% porosity) is close to that of human cancellous bone [19,20]. In addition, the

trend for a higher Young's modulus at lower porosity and higher nanobioglass concentration is reasonable.

The value obtained for Young's modulus proved to be better than the values obtained in other studies. Blaker et al. investigated the mechanical properties of PDLLA/bioglass composite scaffolds. These investigations showed that 15% volume fractions of bioglass microparticles in composite scaffolds can only have a slight trend to stiffening in the composites ($E = 1.29$ MPa), in comparison with pure PDLLA foams ($E = 0.89$ MPa) [21]. Lu et al. also showed that PLGA with 75 wt% bioglass (microparticle) composite scaffolds, which have a porosity of 43% with a mean pore diameter of $89 \mu\text{m}$, possessed an elastic modulus of 51.33 MPa [22]. This amount of Young's modulus is close to the S15 sample's modulus in our study, but S15 possesses a higher porosity (58.9%) with a higher pore diameter ($250\text{--}300 \mu\text{m}$) and has only 10 wt% nanobioglass in its structure. Therefore, when comparing the mechanical properties of composite scaffolds, in this study, nanobioglass, as a reinforcement phase with low mass fraction, can be more effective than micro-materials with high mass fraction, as in other studies [21–24].

The Gibson and Ashby model given by Eq. (3) has generally been applied to relate the modulus to the porosity of foams [18]:

$$\frac{E}{E_0} = C(1 - P)^n, \quad (3)$$

where E and E_0 are the Young's modulus of the foam and non-porous materials, respectively, and P is porosity. Constants C and n depend on the foam microstructure. The value of n generally lies in the range $1 < n < 4$, giving a wide range of values for E/E_0 at a given porosity [25]. It has been suggested that for closed-cell porous systems, n should have a value in the range of $1 < n < 2$. In this study, Eq. (3) was used to predict the interconnectivity of scaffolds, which was assessed by calculating n values based on experimental data. The resultant n values, which were higher than 2, demonstrated the fact that these materials possess interconnected pores.

The tensile strength was measured for scaffolds and the results are displayed in Figure 4. As can be observed, the tensile strength increases significantly with the subtraction of porosity and the addition of nanobioglass. With increasing porosity, however, the apparent scaffold's strength decreases. Sufficient porosity is also essential to reach high permeability for waste removal and nutrient supply to the scaffold from the surrounding healthy bone [26].

The IR transmittance spectra for the PHB/bioglass nanocomposite have been shown in Figure 5 [13] and the bond groups of two phases of nanocomposite have been presented. In the

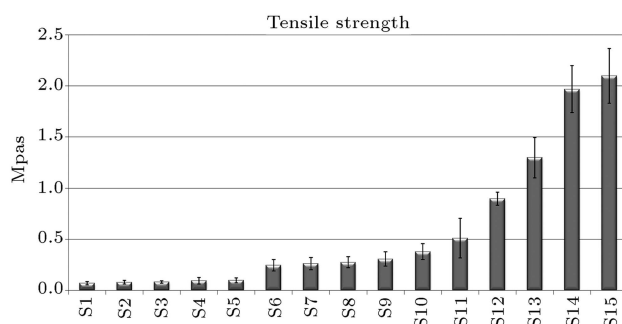


Figure 4. Tensile strength of scaffolds. The data: $n = 3$, error bars = \pm SD.

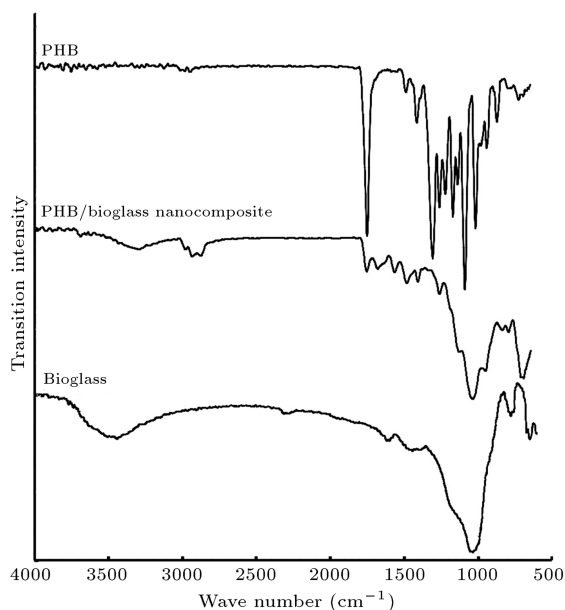


Figure 5. FTIR of bioglass, PHB/bioglass nanocomposite and PHB.

forementioned figure, the peak of the carbonyl groups at 1720 cm^{-1} is smaller than pure PHB. In addition, the peak of the Ca-O bonds at about 650 cm^{-1} is more intense than pure bioglass. It also seems that there is some interaction between nanobioglass and poly (3-hydroxybutyrate), so the bonds at about 760

cm^{-1} may be assigned to CaO with the carbonyl group. Moreover, some peaks are shifted, which gives more reason to believe that the carbonyl group participates in the interaction with CaO. Therefore, it seems that there is a good bond between nanobioglass and poly(3-hydroxybutyrate) in the interface of nanocomposite phases.

In our previous study, the DTA results also showed that there is a favorable interaction between polymer and bioglass nano-particles, which improves the connection in the interface of the nanocomposite phases [13]. Therefore, composite scaffolds become more rigid with the addition of nanobioglass particles.

The results showed that the mechanical properties improved with the addition of nanobioglass, thus, the bioglass nanoparticles fulfilled their reinforcing role. When the bioglass nanoparticles are put into the structure of the PHB scaffold, the pore walls get more rigid and, as a consequence, they do not fracture as easily as in the case of neat PHB scaffolds. Besides, the fact that the mechanical properties have increased, indicates a good initial adhesion between the PHB and the nanobioglass.

3.3. The Bioactivity of scaffolds

The scaffolds containing 10 wt% of nanobioglass prepared in this study were subjected to the *in vitro* bioactivity test by examining the formation of hydroxyapatite on their surfaces after immersion in SBF under normal physiological conditions. After 4 weeks immersion, a thin mineral layer was formed on the surfaces of the PHB/bioglass nanocomposite, which was investigated by SEM, as shown in Figure 6(a)-(c). These images were taken in the backscattered condition to increase contrast between the mineral phase and the scaffold surface. The Ca/P molar ratio of the apatite agglomerate was determined by EDS analysis as ~ 1.6 , similar to the standard Ca/P ratio of 1.67 of stoichiometric hydroxyapatite (Figure 6(d)). The EDS results demonstrated that the mineral phase formed on the surface was hydroxyapatite. In contrast, the neat PHB scaffolds had no changes on the surface after 4

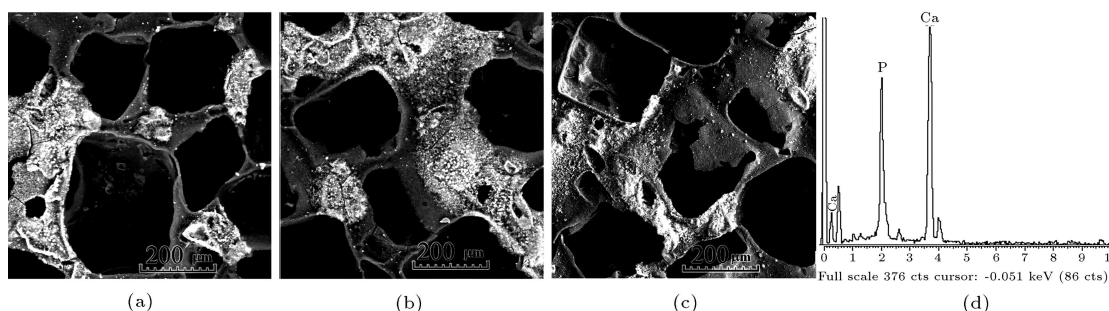


Figure 6. Hydroxyapatite formed on the nanocomposite scaffold after 4 week in SBF: (a) The scaffold was prepared by 90 wt% NaCl; (b) the scaffold was prepared by 80 wt% NaCl; (c) the scaffold was prepared by 70 wt% NaCl; (d) EDS analysis of the nanocomposite scaffold after immersion in SBF for 4 weeks.

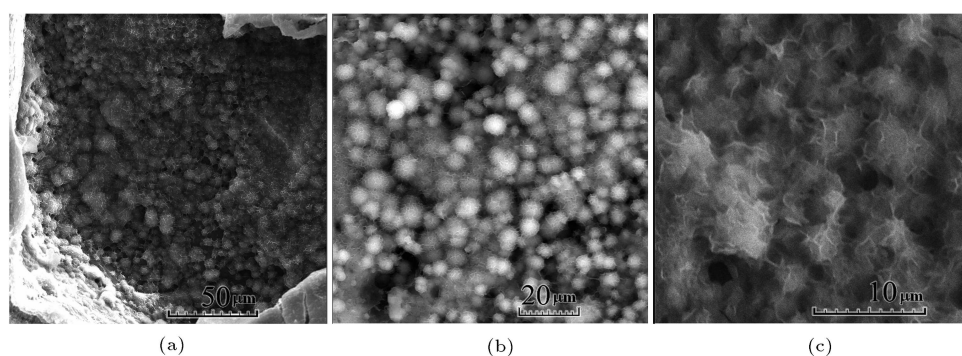


Figure 7. Hydroxyapatite formed on the nanocomposite scaffold with (a) 800 × magnification, (b) 1350 × magnification and (c) 5000 × magnification.

weeks of immersion and no evidence of bioactivity was recorded.

The nanocomposite scaffolds were investigated using SEM under higher magnification, in order to observe the formed hydroxyapatite in more detail, and the results have been shown in Figure 7. It can be seen that the particles formed *in vitro* have a spherical shape, which is similar to the shape of hydroxyapatite formation in some bioactivity studies [27–29].

As mentioned by Kokubo and Takadama [14], apatite formation on the surface of a material in SBF showed that the material can bond to living bone through the apatite layer formed on its surface in the living body, and predict the degree of *in vivo* bone bioactivity of the material. Therefore, it can be predicted that when these nanocomposite scaffolds are implanted in the body, they will have a favorable bonding with the bone and induce bone reconstruction in the scaffolds by nucleation of hydroxyapatite on its surfaces. Therefore, the nanobioglass not only improves mechanical properties, but also provides a bioactive character to the nanocomposite scaffolds.

4. Conclusion

In this study, different weight ratios of nanobioglass (0, 2.5, 5, 7.5 and 10 wt%) reinforced poly(3-hydroxybutyrate) composite scaffolds with various porosity (70, 80 and 90 wt% of NaCl) were successfully prepared via the salt leaching process. The mechanical and bioactivity properties of the scaffolds were evaluated for bone tissue engineering. The greater specific surface area of the bioglass nanoparticles should lead to increased interface effects, and should also cause improved bioactivity and increased mechanical properties of scaffolds. The results showed that by decreasing the volume fraction of porosity and increasing the bioglass nanoparticles, Young's modulus and the tensile strength of scaffolds were improved significantly. It is also possible to optimize the scaffold for bone tissue engineering application by variation of porosity

and the needed mechanical properties. In conclusion, bioactive scaffolds were designed with a wide range of mechanical properties that can be used for bone tissue engineering.

References

- Salgado, A.J., Coutinho, O.P. and Reis, R.L. "Bone tissue engineering: state of the art and future trends", *Macromol. Biosci.*, **4**, pp. 743-765 (2004).
- Chen, G.Q. and Wu, Q. "The application of polyhydroxyalkanoate as tissue engineering materials", *Biomaterials*, **26**, pp. 6565-6578 (2005).
- Galego, N., Rozsa, C., Sanchez, R., Fung, J., Vazquez, A. and Tomas, J.S. "Characterization and application of poly (b-hydroxyalkanoates) family as composite biomaterials", *Polym. Test.*, **19**, pp. 485-492 (2000).
- Misra, S.K., Valappil, S.P., Roy, I. and Boccaccini, A.R. "Polyhydroxyalkanoate (PHA)/inorganic phase composites for tissue engineering applications", *Biomacromolecules*, **7**, pp. 2249-2258 (2006).
- Misra, S.K., Mohn, D., Brunner, T.J., Stark, W.J., Philip, S.E., Roy, I., Salih, V., Knowles, J.C. and Boccaccini, A.R. "Comparison of nanoscale and microscale bioactive glass on the properties of P(3HB)/bioglass composites", *Biomaterials*, **29**, pp. 1705-1761 (2008).
- Wei, G. and Ma, P.X. "Structural and properties of nano-hydroxyapatite/ polymer composite scaffolds for bone tissue engineering", *Biomaterials*, **25**, pp. 4749-4757 (2004).
- Misra, S.K., Nazhat, S.N., Valappil, S.P., Torbati, M.M., Wood, R.J.K., Roy, I. and Boccaccini, A.R. "Fabrication and characterization of biodegradable poly (3-hydroxybutyrate) composite containing bioglass", *Biomacromolecules*, **8**, pp. 2112-2119 (2007).
- Ginebra, M.P., Driessens, F.C.M. and Planell, J.A. "Effect of the particle size on the micro and nanostructural features of calcium phosphate cement: a

- kinetic analysis”, *Biomaterials*, **25**, pp. 3453-3462 (2004).
9. Nejati, E., Mirzadeh, H. and Zandi, M. “Synthesis and characterization of nano-hydroxyapatite rods/poly (L-lactide acid) composite scaffolds for bone tissue engineering”, *Composites*, **39**, pp. 1589-1596 (2008).
 10. Boccaccini, A.R., Erol, M., Stark, W.J., Mohn, D., Hong, Z. and Mano, J.F. “Polymer/bioactive glass nanocomposites for biomedical applications: A review”, *Compos. Sci. Technol.*, **70**, pp. 1764-1776 (2010).
 11. Palin, E., Liu, H.N. and Webster, T.J. “Mimicking the nanofeatures of bone increases bone-forming cell adhesion and proliferation”, *Nanotechnology*, **16**, pp. 1828-1835 (2005).
 12. Fathi, M.H. and Doostmohammadi, A. “Bioactive glass nanopowder and bioglass coating for biocompatibility improvement of metallic implant”, *J. Mater. Process. Tech.*, **209**, pp. 1385-1391 (2009).
 13. Hajiali, H., Karbasi, S., Hosseinalipour, M. and Rezaie, H.R. “Preparation of a novel biodegradable nanocomposite scaffold based on poly (3-hydroxybutyrate)/bioglass nanoparticles for bone tissue engineering”, *J. Mater. Sci.: Mater. Med.*, **21**, pp. 2135-2132 (2010).
 14. Kokubo, T. and Takadama, H. “How useful is SBF in predicting in vivo bone bioactivity?”, *Biomaterials*, **27**, pp. 2907-2915 (2006).
 15. Murphy, C.M., Haugh, M.G. and O'Brien, F.J. “The effect of mean pore size on cell attachment, proliferation and migration in collagen-glycosaminoglycan scaffolds for bone tissue engineering”, *Biomaterials*, **31**, pp. 461-466 (2010).
 16. Oh, S.H., Park, K., Kim, J.M. and Lee, J.H. “In vitro and in vivo characteristics of PCL scaffolds with pore size gradient fabricated by a centrifugation method”, *Biomaterials*, **28**, pp. 1664-1671 (2007).
 17. Petite, H. and Quarto, R. “Engineered bone”, *Tissue Engineering of Bone*, available at <http://www.Eurekah.com> (2005).
 18. Gibson, L.G. and Ashby, M.F., *Cellular Solids*, Perg Mon Press, Oxford (1988).
 19. Giesen, E.B.W., Ding, M., Dalstra, M. and Eijden, T.M.G.J. “Mechanical properties of cancellous bone in the human mandibular condyle are anisotropic”, *J. Biomech.*, **34**, pp. 799-803 (2001).
 20. Yeni, Y.N. and Fyhrie, D.P. “Finite element calculated uniaxial apparent stiffness is a consistent predictor of uniaxial apparent strength in human vertebral cancellous bone tested with different boundary conditions”, *J. Biomech.*, **34**, pp. 1649-1654 (2001).
 21. Blaker, J.J., Maquet, V., Jerome, R., Boccaccini, A.R. and Nazhat, S.N. “Mechanical properties of highly porous PDLA/Bioglass composite foams as scaffolds for bone tissue engineering”, *Acta Biomater.*, **1**, pp. 643-652 (2005).
 22. Lu, H.H., El-Amin, S.F., Scott, K.D. and Laurencin, C.T. “Three-dimensional, bioactive, biodegradable, polymer-bioactive glass composite scaffolds with improved mechanical properties support collagen synthesis and mineralization of human osteoblast-like cells *in vitro*”, *J. Biomed. Mater. Res.*, **64A**, pp. 465-474 (2003).
 23. Zhang, R.Y. and Ma, P.X. “Poly (alpha-hydroxyl acids)/hydroxyapatite porous composites for bone-tissue engineering. I. Preparation and morphology”, *J. Biomed. Mater. Res.*, **44**, pp. 446-455 (1999).
 24. Guan, L. and Davies, J.E. “Preparation and characterisation of a highly macroporous biodegradable composite tissue engineering scaffold”, *J. Biomed. Mater. Res.*, **71A**, pp. 480-487 (2004).
 25. Roberts, A.P. and Garboczi, E.J. “Elastic moduli of model random threedimensional closed-cell cellular solids”, *Acta Mater.*, **49**, pp. 189-197 (2001).
 26. Sanz-Herrera, A., Garcia-Aznar, J.M., Doblare, M. “A mathematical model for bone tissue regeneration inside a specific type of scaffold”, *Biomech. Model. Mechan.*, **7**, pp. 355-366 (2008).
 27. Kim, H.M., Miyaji, F., Kokubo, T. and Nakamura, T. “Preparation of bioactive Ti and its alloys via simple chemical surface treatment”, *J. Biomed. Mater. Res.*, **32**, pp. 409-417 (1996).
 28. Li, P., Ohtsuki, C., Kokubo, T., Nakanishi, K., Soga, N., Nakamura, T. Yamamuro, T. “Apatite formation induced on silica gel in a simulated body fluid”, *J. Am. Ceram. Soc.*, **75**, pp. 2094-2097 (1992).
 29. Li, P., Ohtsuki, C., Kokubo, T., Nakanishi, K., Soga, N. and de Groot, K. “A role of hydrated silica, titania and alumina in forming biologically active bone-like apatite on implant”, *J. Biomed. Mater. Res.*, **28**, pp. 7-15 (1994).

Biographies

Hadi Hajiali received a BS degree in Prosthetics from Isfahan University of Medical Sciences, Iran, in 2007, and an MS degree in Biomedical Engineering (Biomaterials) from Iran University of Science and Technology, in 2010. He is currently pursuing research in Biomedical Engineering with special interest in regenerative medicine, tissue engineering, advanced biomaterials and nanobiotechnology.

Saeed Karbasi received his BS degree in Material Engineering from Shiraz University, Iran, in 1994, and MS and PhD degrees in Biomedical Engineering from Amirkabir University, Iran, in 1997 and 2007, respectively. He is currently Associate Professor at Isfahan

University of Medical Sciences, Iran. His research interests include biomaterials, tissue engineering and nanobiomaterials.

Mohammad Hosseinalipour received his MD in Clinical and Surgical Pathology from Iran University of Medical Sciences, and is currently Assistant Professor at Iran University of Science and Technology, Iran. His research interests include biomaterials, biocompatibil-

ity of materials and tissue engineering.

Hamid Reza Rezaie received his PhD degree in Ceramics from the University of Sheffield, UK, in 1998, and is currently Professor in the School of Metallurgy & Materials Engineering at Iran University of Science and Technology, Iran. His research interests include ceramics, refractories, raw materials and traditional ceramics.